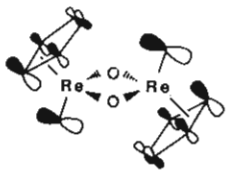

F

to the extent of the oxo ligand. For example, Cp^*ReOCl_2 displays a similar "slipped" Cp* ring, *toward* the Cl ligands.[51] This effect can be attributed to the very short M–O bond lengths for terminal oxo ligands, thus forcing their lone pairs closer to the Cp* π orbitals.

Acknowledgment. We gratefully acknowledge Professor W. A. Herrmann for communication of results prior to publication.

Appendix

Molecular orbital calculations were performed on an IBM 3081-D computer system using the Fenske–Hall approximate MO method.[55] The atomic positions for *trans*-**1**,[11] **2**,[10] **4**,[7] and **5**[12] were taken from their crystal structures and idealized to C_{2h}, C_{2v}, C_{2v}, and C_{2h} symmetry, respectively. All η^5-C_5R_5 rings were modeled by using η^5-C_5H_5 rings. Local D_{5h} symmetry was invoked upon the cyclopentadienyl rings, and a C–H distance of 1.08 Å was used for each calculation. In step a of Scheme I the surface was modeled by varying the Mo–Mo–S_t and Mo–Mo–Cp(centroid) angles as well as the Mo–Mo and Mo–S distances in a linear fashion. In step b, the symmetric $(\mu\text{-S})_4$ core was transformed into that of **2** by varying the S–S distances linearly. In step c, the Mo–Mo–S_t and Mo–Mo–Cp(centroid) angles were varied linearly. In step d, the dihedral angle between the Mo–(μ-S)–Mo bridge planes, ϕ, as well as the Mo–Mo and Mo–S distances were varied linearly such that the atomic positions in *cis*-**1** were the same as in *trans*-**1** after rotating one CpMoS fragment through 180° about the Mo–Mo vector. The potential surface illustrated in Figure 7 for compound **4** was generated by varying only the dihedral angle, ϕ, between the Mo–(μ-O)–Mo bridge planes. The potential surface modeled in Figure 8 was generated by varying the Re–Re distance from 2.74 to 3.54 Å and the (μ-O)···(μ-O) distance from 2.34 to 1.67 Å without varying any other bond lengths. The tetrahydrido frameworks used in Figures 1 and 6 were constructed from the interatomic angles of *trans*-**1** and **4**, respectively, by assuming the following bond lengths: Mo–H_t = 1.80 Å, Mo–(μ-H) = 1.90 Å.

All atomic wavefunctions were generated by using the method of Bursten, Jensen, and Fenske.[56] Contracted double-ζ representations were used for the Re 5d, Mo 4d, S 3p, C 2p, and O 2p AO's. An exponent of 1.16 was used for the H 1s AO.[57] The basis functions for Re and Mo were derived for the +3 oxidation state (s^0d^n) with the following fixed exponents: Re, 2.0 (6s), 1.8 (6p); Mo, 2.0 (5s), 1.6 (5p). For the C_5H_5 ligand, the first three occupied orbitals were filled with 2.0 electrons and deleted from the basis transformation set, and all virtual orbitals above the e_2'' level (D_{5h}) were filled with 0.0 electron and deleted from the basis transformation set in all calculations.[58] The C_5H_5 ligands were converged as the monoanion, the *molecular* orbitals of which were allowed to interact with the metal centers. All calculations were converged with a self-consistent-field iterative technique using a convergence criteria of 0.0010 as the largest deviation of atomic orbital populations between successive cycles.

(56) Bursten, B. E.; Jensen, J. R.; Fenske, R. F. *J. Chem. Phys.* **1978**, *68*, 3320–3321.
(57) Hehre, W. J.; Stewart, R. F.; Pople, J. A. *J. Chem. Phys.* **1969**, *51*, 2657–2664.
(58) Lichtenberger, D. L.; Fenske, R. F. *J. Chem. Phys.* **1976**, *64*, 4247–4264.

Contribution from the Istituto di Strutturistica Chimica "G. Giacomello", Area della Ricerca di Roma, CNR, C.P. 10, 00016 Monterotondo Stazione, Roma, Italy, and Istituto di Chimica, Università di Ferrara, via L. Borsari, 46, Ferrara, Italy

Stable Paramagnetic Dihydrido Complexes of Iridium(IV): Synthesis, X-ray Crystal Structure, and Behavior in Solution of $Ir^{IV}(H)_2(Cl)_2(P\text{-}i\text{-}Pr_3)_2$ (1) and $Ir^{IV}(H)_2(Cl)_2(PCy_3)_2$ (2)[1]

Pasquale Mura,* Annalaura Segre, and Silvana Sostero

Received October 17, 1988

The 17-electron dihydrido complexes of iridium(IV) $Ir^{IV}(H)_2(Cl)_2(P\text{-}i\text{-}Pr_3)_2$ (**1**) and $Ir^{IV}(H)_2(Cl)_2(PCy_3)_2$ (**2**) are prepared by the reaction of $(NH_4)_2IrCl_6$ with PR_3 (PR_3 = P-*i*-Pr_3 and PCy_3) in refluxing ethanol, containing concentrated HCl. Their magnetic moments are 1.5 and 1.6 μ_B, respectively. The crystal structures of **1** and **2** reveal slightly distorted octahedral geometries with three pairs of trans ligands: PR_3, Cl, and H. Contrary to all expectations, **1** and **2** give sharp, well-resolved ^1H NMR spectra in $CDCl_3$ solutions with hydride chemical shifts at extremely high field (δ = −49.0 (t) and −47.9 (t) ppm, respectively). A very unusual temperature-dependent solution equilibrium between paramagnetic and diamagnetic species involving molecular hydrogen is proposed for both complexes.

Introduction

Very few paramagnetic hydrides of transition metals are known,[2] and most of them, due to poor stability, have been characterized only in solution at low temperature by electron spin resonance spectroscopy.[3,4] To our knowledge, only two mononuclear tantalum[4] complexes, one cobalt[5] complex, and one binuclear rhodium[6] complex were sufficiently stable to allow the determination of their X-ray crystal structures.

Paramagnetic iridium(IV) complexes are stable and have been extensively investigated.[7] Furthermore, iridium easily forms hydrido compounds in the formal oxidation states I, III, and V.[8,9] Recently we reported the synthesis, X-ray crystal structure, and solution behavior of the first example of a paramagnetic hydrido

* To whom correspondence should be addressed at the Istituto di Strutturistica Chimica "G. Giacomello".

(1) Presented in part at the 3rd International Conference on the Chemistry of the Platinum Group Metals, Sheffield, U.K., July 13, 1987, and at the 20th Congresso Nazionale di Chimica Inorganica, Pavia, Italy, Sept 15, 1987.
(2) (a) Rhodes, L. F.; Zubkowski, J. D.; Folting, K.; Huffman, J. C.; Caulton, K. G. *Inorg. Chem.* **1982**, *21*, 4185–4192 and references cited therein. (b) Rhodes, L. F.; Caulton, K. G. *J. Am. Chem. Soc.* **1985**, *107*, 259–260 and references cited therein.
(3) Allison, J. D.; Walton, R. A. *J. Am. Chem. Soc.* **1984**, *106*, 163–168 and references cited therein.
(4) Luetkens, M. L., Jr.; Elcesser, W. L.; Huffman, J. C.; Sattelberger, A. P. *Inorg. Chem.* **1984**, *23*, 1718–1726 and references cited therein.
(5) Bianchini, C.; Masi, D.; Mealli, C.; Meli, A.; Sabat, M. *Gazz. Chim. Ital.* **1986**, *116*, 201–206.

0020-1669/89/1328-2853$01.50/0

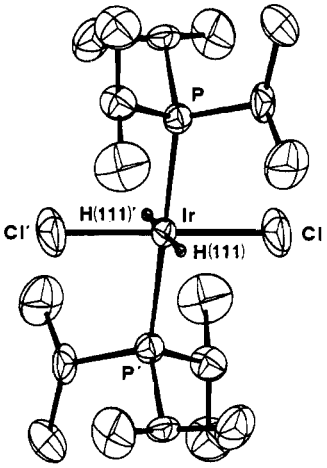

Figure 1. Geometry[29] of the $Ir^{IV}(H)_2(Cl)_2(P\text{-}i\text{-}Pr_3)_2$ molecule with hydrogen atoms of the P-*i*-Pr_3 groups omitted for clarity. The Ir atom occupies the position of crystallographic symmetry $\bar{1}$. Thermal ellipsoids are drawn at the 50% probability level.

complex of platinum-group metals, $Ir^{IV}(H)_2(Cl)_2(P\text{-}i\text{-}Pr_3)_2$ (**1**).[10,11] In view of the stability of this compound, we thought that by using appropriate phosphine ligands the method used to prepare **1** might provide a general synthesis of paramagnetic iridium dihydrides. Indeed, we have synthesized the paramagnetic dihydrido complex $Ir^{IV}(H)_2(Cl)_2(PCy_3)_2$ (**2**). Here we report in full the syntheses, properties, and X-ray crystal structures of **1**[10,11] and **2**.

Results and Discussion

Synthesis and Solid-State Properties of $Ir^{IV}(H)_2(Cl)_2(P\text{-}i\text{-}Pr_3)_2$ (1) and $Ir^{IV}(H)_2(Cl)_2(PCy_3)_2$ (2). The formally 17-electron complexes **1** and **2** are prepared in appreciable yield from $(NH_4)_2IrCl_6$ by reacting a suspension of $(NH_4)_2IrCl_6$ with the phosphine (P-*i*-Pr_3 (**1**) and PCy_3 (**2**)) in ethanol containing concentrated HCl. A solid remains in suspension throughout the reaction; however, several color changes occur as the reaction proceeds. When the filtered precipitates are washed with water, pure samples of deep red **1** or red-violet **2** are obtained. The nature of the phosphine is critical to the success of the preparation; less bulky phosphines such as PPh_3 give complexes containing three phosphine ligands.[12]

Elemental analyses[13] of **1** and **2** are consistent with the presence of two phosphine groups and two chlorine atoms. Molecular weight determinations show that both compounds are present as monomeric species in benzene (**1**) or chloroform (**2**) solutions.

Attempts to confirm the molecular structure of the solids by infrared spectroscopy gave ambiguous results. Thus, the spectra of **1** and **2** in KBr pellets showed the presence of fairly weak bands in the region of terminal M–H bonds, i.e., 2116 (w, sharp)[14] and 2002 cm^{-1} (mw, sharp) for **1** and 2001 cm^{-1} (w, broad) for **2**. These are accompanied by a broad region of absorption at ca. 1620 cm^{-1}. However, the intensity of the bands is unusually sensitive toward pellet preparation; moreover, these bands are not observed when the spectra of Nujol mulls are recorded.[15] Attempts to

Table I. Atomic Coordinates and Isotropic Thermal Parameters ($Å^2$) with Their Esd's in Parentheses for $Ir^{IV}(H)_2(Cl)_2(P\text{-}i\text{-}Pr_3)_2$ (**1**)

	x	*y*	*z*	*B*(eq)[a]
Ir(1)	0.0000	−0.5000	0.5000	2.444 (3)
Cl(1)	−0.0147 (2)	−0.3073 (1)	0.4040 (1)	6.20 (4)
P(1)	0.1262 (1)	−0.3377 (1)	0.5974 (1)	2.57 (1)
C(1)	0.2601 (6)	−0.4329 (5)	0.6756 (3)	3.0 (1)
C(2)	0.2370 (6)	−0.1811 (5)	0.5520 (3)	3.9 (1)
C(3)	−0.0286 (5)	−0.2440 (5)	0.6579 (3)	3.5 (1)
C(11)	0.398 (1)	−0.521 (1)	0.6365 (6)	7.3 (2)
C(12)	0.331 (1)	−0.3393 (9)	0.7466 (4)	6.3 (2)
C(21)	0.298 (1)	−0.0572 (8)	0.6089 (5)	6.0 (2)
C(22)	0.3728 (9)	−0.234 (1)	0.4985 (5)	6.6 (2)
C(31)	−0.1377 (9)	−0.142 (1)	0.6059 (5)	5.0 (2)
C(32)	−0.1285 (9)	−0.3568 (8)	0.7035 (4)	5.6 (2)
H(111)	0.231 (9)	−0.516 (9)	0.499 (4)	1 (2)

[a] $B(\text{eq}) = {}^4/_3\sum_{ij}[A_iA_jB_{ij}]$.

Table II. Atomic Coordinates and Isotropic Thermal Parameters ($Å^2$) with Their Esd's in Parentheses for $Ir^{IV}(H)_2(Cl)_2(PCy_3)_2$ (**2**)

	x	*y*	*z*	*B*(eq)[a]
Ir(1)	0.0000	0.5000	0.5000	2.069 (4)
Cl(1)	0.1470 (1)	0.5651 (1)	0.3952 (1)	4.31 (3)
P(1)	0.2030 (1)	0.5312 (1)	0.7070 (1)	2.17 (2)
C(111)	0.2551 (3)	0.3564 (3)	0.6980 (3)	2.6 (1)
C(112)	0.1454 (4)	0.2599 (3)	0.7115 (4)	3.6 (1)
C(113)	0.1965 (4)	0.1196 (4)	0.7051 (4)	4.2 (1)
C(114)	0.2238 (4)	0.0394 (3)	0.5656 (4)	4.1 (1)
C(115)	0.3333 (4)	0.1337 (4)	0.5524 (4)	4.3 (1)
C(116)	0.2853 (4)	0.2748 (3)	0.5582 (3)	3.7 (1)
C(121)	0.1691 (3)	0.6096 (3)	0.8795 (2)	2.6 (1)
C(122)	0.1061 (4)	0.7477 (4)	0.9041 (3)	3.7 (1)
C(123)	0.0567 (4)	0.7869 (4)	1.0336 (4)	4.4 (1)
C(124)	0.1770 (4)	0.7993 (4)	1.1713 (3)	4.5 (1)
C(125)	0.2415 (4)	0.6649 (4)	1.1456 (3)	4.2 (1)
C(126)	0.2943 (3)	0.6278 (4)	1.0186 (3)	3.5 (1)
C(131)	0.3709 (2)	0.6337 (3)	0.7264 (3)	2.6 (1)
C(132)	0.3683 (3)	0.7937 (3)	0.7695 (4)	3.7 (1)
C(133)	0.4942 (4)	0.8654 (5)	0.7529 (6)	5.2 (2)
C(134)	0.6383 (4)	0.8436 (5)	0.8417 (6)	5.4 (2)
C(135)	0.6401 (3)	0.6865 (4)	0.8036 (5)	4.6 (1)
C(136)	0.5150 (3)	0.6149 (4)	0.8209 (4)	3.7 (1)
H(111)	0.006 (9)	0.34 (1)	0.42 (1)	14 (2)

[a] See footnote *a* of Table I.

Table III. Relevant Bond Distances (Å) and Angles (deg) for $Ir^{IV}(H)_2(Cl)_2(P\text{-}i\text{-}Pr_3)_2$ (**1**)

Ir–Cl	2.342 (1)	Ir–H(111)	1.90 (7)
Ir–P	2.360 (1)		
Cl–Ir–P	90.27 (4)	P–Ir–H(111)	70 (2)
Cl–Ir–H(111)	93 (2)		

Table IV. Relevant Bond Distances (Å) and Angles (deg) for $Ir^{IV}(H)_2(Cl)_2(PCy_3)_2$ (**2**)

Ir–Cl	2.342 (1)	Ir–H(111)	1.56 (14)
Ir–P	2.362 (1)		
Cl–Ir–P	91.12 (3)	P–Ir–H(111)	93 (5)
Cl–Ir–H(111)	90 (3)		

(6) Bianchini, C.; Mealli, C.; Meli, A.; Sabat, M. *J. Chem. Soc., Chem. Commun.* **1986**, 777–779.
(7) (a) Chatt, J.; Leigh, G. J.; Mingos, D. M. P.; Paske, R. J. *J. Chem. Soc. A* **1968**, 2636–2641 and references cited therein. (b) Fergusson, J. E.; Rankin, D. A. *Aust. J. Chem.* **1983**, *36*, 863–869 and references cited therein. (c) Rankin, D. A.; Penfold, B. R.; Fergusson, J. E. *Ibid.* **1983**, *36*, 871–883 and references cited therein. (d) Isobe, K.; Vazquez de Miguel, A.; Nutton, A.; Maitlis, P. M. *J. Chem. Soc., Dalton Trans.* **1984**, 929–933 and references cited therein.
(8) For general reviews, see: (a) Muetterties, E. L., Ed. *Transition Metal Hydrides*; Marcel Dekker: New York, 1971. (b) Bau, R., Ed. *Adv. Chem. Ser.* **1978**, *No. 167*. (c) Teller, R. G.; Bau, R. *Struct. Bonding (Berlin)* **1981**, *44*, 1–82.
(9) Gomez, M.; Robinson, D. J.; Maitlis, P. M. *J. Chem. Soc., Chem. Commun.* **1983**, 825–826 and references cited therein.
(10) Mura, P. *J. Am. Chem. Soc.* **1986**, *108*, 351–352.
(11) Mura, P.; Segre, A. *Angew. Chem., Int. Ed. Engl.* **1986**, *25*, 460–462.
(12) Shaw, B. L.; Stainbank, R. E. *J. Chem. Soc., Dalton Trans.* **1972**, 2108–2112 and references cited therein.
(13) Anal. Calcd (found) for $Ir^{IV}(H)_2(Cl)_2(P\text{-}i\text{-}Pr_3)_2$ (**1**, $C_{18}H_{44}Cl_2P_2Ir$): C, 36.91 (34.90); H, 7.59 (7.00); Cl, 12.11 (12.16); P, 10.58 (10.75). Calcd for $Ir^{IV}(H)_2(Cl)_2(PCy_3)_2$ (**2**, $C_{36}H_{68}Cl_2P_2Ir$): C, 52.34 (52.25); H, 8.31 (8.32); Cl, 8.58 (8.76); P, 7.50 (7.26). Elemental analyses were carried out by "Servizio di Microanalisi" of the Research Area of Rome.

(14) In the preliminary communication (see ref 10), we did not mention this band because, although present, it was very weak and therefore was difficult to attribute. A more accurate collection of IR spectra, on several samples, gives us the ability to detect the presence of this band without any doubt.

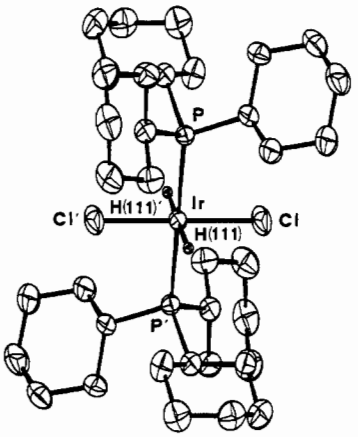

Figure 2. Geometry[29] of the $Ir^{IV}(H)_2(Cl)_2(PCy_3)_2$ molecule with hydrogen atoms of the PCy_3 groups omitted for clarity. The Ir atom occupies the position of crystallographic symmetry $\bar{1}$. Thermal ellipsoids are drawn at the 50% probability level.

prepare the D_2 analogue of **1** led to the formation of the corresponding compound in which extensive deuteriation of the organic ligands had occurred. The bands due to these deuteriated ligands masked the hydride region. In addition, in the far-IR spectra **1** and **2** show strong sharp bands at 317.5 (s) and 317 cm^{-1} (s), respectively, in agreement with the presence of trans chlorine atoms.[16]

The magnetic moments μ_{eff} of **1** and **2**, at room temperature, are 1.5 and 1.6 μ_B, respectively; this is in agreement with a spin-paired d^5 electron configuration (low-spin Ir(IV)).[16,17] Thus, **1** and **2** are formally 17-electron hydride complexes. Compound **1** showed only one broad unresolved resonance in the solid-state EPR spectrum down to 95 K, in addition to detectable traces of an unknown impurity.[18]

The solid-state EPR spectrum of **2** at 95 K shows again a broad resonance together with detectable traces of an unknown impurity.[18]

Molecular Structures. Figures 1 and 2 show perspective views of $Ir^{IV}(H)_2(Cl)_2(P\text{-}i\text{-}Pr_3)_2$ (**1**) and $Ir^{IV}(H)_2(Cl)_2(PCy_3)_2$ (**2**), respectively, and define the atom-numbering scheme for the heavy and hydride hydrogen atoms. Final positional parameters are given in Tables I and II. Selected bond lengths and angles are given in Tables III and IV. A listing of thermal parameters, hydrogen atomic parameters, and observed and calculated structure factors is available as supplementary material. The crystal structures of **1** and **2** consist of discrete molecules. The geometry around the iridium atom in both complexes is that of a slightly distorted octahedron, with three pairs of trans ligands: PR_3, Cl, and H. The Ir atom occupies the position of crystallographic symmetry $\bar{1}$; half of the molecule is contained in the asymmetric unit. All the atoms, including the hydride ligands and the hydrogen atoms of the organic ligands, were located and refined satisfactorily to R_F values of 0.0312 and 0.0181 for **1** and **2**, respectively. The Ir–H distances in **1** and **2** are 1.90 (7) and 1.56 (14) Å, respectively, values that are in agreement with others reported in the literature.[19]

Behavior in Solution of $Ir^{IV}(H)_2(Cl)_2(P\text{-}i\text{-}Pr_3)_2$ (1) and $Ir^{IV}(H)_2(Cl)_2(PCy_3)_2$ (2). A ^1H and ^{31}P NMR study of solutions of these complexes shows that they are not predominantly species A in solution but that the major components are of a different type, B (see reaction a). The ^1H NMR spectra ($CDCl_3$, 298 K

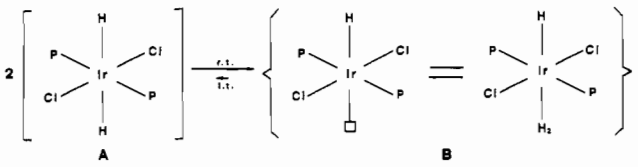

(a)

in reference to TMS) of **1** and **2** (see Figure 3 for compound **2** and ref 11 for compound **1**) contain sharp, well-resolved multiplets. Relative intensities for **1** are 6:36:1; δ(PCH) = 3.11 (m) ppm, $\delta(PCHCH_3)$ = 1.33 (d, vt) ppm, and δ(IrH) = −49.0 (t) ppm;[20] $J(HH)$ = 7.3 Hz and $J(PH_{hydride})$ = 11.1 Hz. Relative intensities for compound **2** are 6:60:1; δ(PCH) = 2.77 (m) ppm, $\delta(CH_2)$ = 1–2 ppm, and δ(IrH) = −47.9 (t) ppm;[20] $J(PH_{hydride})$ = 11.0 Hz.

Another very broad peak, centered at ~2.5 ppm for **1** and at ~−0.4 ppm, much less broad, for **2**, is also always present and will be discussed below.

The broad-band decoupled $^{31}P\{^1H\}$ spectra (C_6D_6, 298 K) show a sharp singlet at δ = 33.08 ppm (relative to 85% H_3PO_4, external reference) and δ = 35.79 ppm for **1** and **2**, respectively. Selective decoupling of the signals due to the protons in the region δ = 1–3 ppm (CH and CH_3 for **1** and CH and CH_2 for **2**) converted those singlets into *doublets*. Thus, it follows from the observed spectra that a *monohydride* with a stereochemistry such as that of compound B is present in solution (reaction a).

It must be noted that the coupling constants, chemical shifts, and relative intensities of the signals are reconcilable only with the presence of a diamagnetic monohydrido complex such as B, which is in complete contrast with the X-ray structure data and magnetic susceptibility measurements performed on solid **1**[10] and **2**.

However, when the temperature is lowered, all peaks of the ^1H and ^{31}P NMR spectra of **1** and **2** broaden noticeably, and at 223 and 213 K for **1** and **2**, respectively, the hydrido peak disappears. A study of the ^1H NMR spectra of **1** and **2** as a function of the temperature was also performed. When the temperature is lowered to 183 K (in CD_2Cl_2 solution), the spectra progressively broaden. This process is reversible. Furthermore, the hydride as well as the methyne signals undergo paramagnetic shifts (Figures 4 and 5). At the same time the solvent peak also slightly broadens. The hysteresis pattern apparent in Figure 4 is most probably due to the fact that only 15 min was given between one NMR run and the other. As solutions of **1** are not stable indefinitely, a new spectrum was run as soon as the temperature was stabilized. Consequently, kinetic reasons can explain the apparent hysteresis cycle, which is observable only for signals due to **1** and not, for instance, for the H_2O signal (water is present as an impurity in solution). The H_2O impurity, always present in $CDCl_3$, does not appreciably affect the proposed equilibrium; in CD_2Cl_2 the equilibrium is about the same. In the case of the analogue **2** with cyclohexyl groups, the same experiment does not show any evidence of the hysteresis pattern, thus suggesting that kinetic reasons can indeed explain the behavior of **1**. It is to be noted that the paramagnetic shift is much more evident for compound **1**.

Since in CD_2Cl_2 we observed a ^{31}P NMR resonance at 183 K, even if it is rather broad, the equilibrium in solution must be strongly shifted toward the diamagnetic species; thus, the rate of the paramagnetic/diamagnetic equilibrium cannot be measured by this method.

Thus, it is reasonable to postulate that an equilibrium between paramagnetic and diamagnetic species exists in solution. The paramagnetic dihydrido species A (reaction a) is present only in trace amounts at 298 K as evidenced by the fact the NMR hydride signal is quite sharp and well resolved. It is worthy of note, however, that inversion-recovery experiments at 298 K, necessary

(15) It should also be added that when powdered samples of **1** and **2** are dried under vacuum, at some point one observes an almost explosive scattering of the sample in the evacuated vessel. This might be due to sudden gas evolution. Thus, it is conceivable that such a transformation could occur, at least in part, during pellet or mull preparation. The above behavior may be also due to solvent removal.

(16) Bennet, M. A.; Milner, D. L. *J. Am. Chem. Soc.* **1969**, *91*, 6983–6994 and references cited therein.

(17) Figgis, B. N. *Introduction to Ligand Fields*; Wiley: New York, 1966; pp 305–306.

(18) Attanasio, D.; Maldotti, A.; Mura, P.; Sostero, S. Manuscript in preparation.

(19) Teller, R. G.; Bau, R. *Struct. Bonding (Berlin)* **1981**, *44*, 1–82 and references cited therein.

(20) Small differences in the hydride chemical shifts are observed when different stocks of $CDCl_3$ are used.

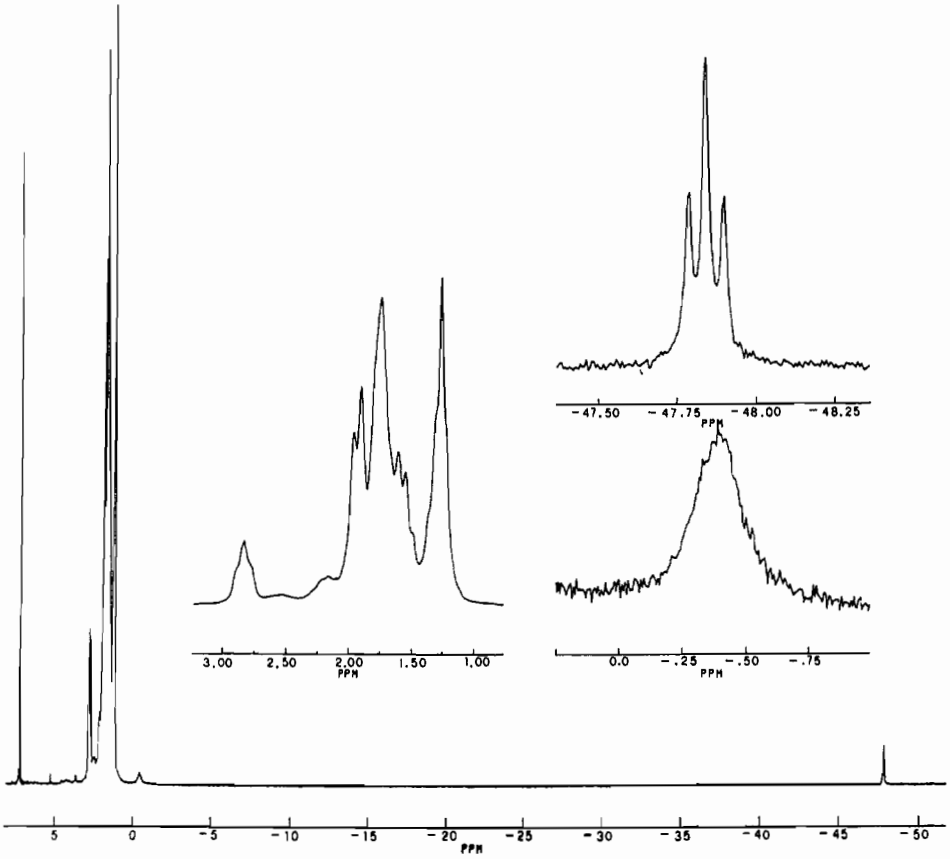

Figure 3. ^1H NMR spectrum of **2** (200 MHz, $CDCl_3$ solution).

for T_1 measurement, performed with the shortest possible τ value between the π and $\pi/2$ pulses (10 ms) do not show any signal inversion. Thus, T_1 must be rather short, consistent with the presence of form A in the equilibrium. At low temperatures the amount of form A increases; thus, T_2 strongly decreases and the hydride signal is too broad to be observed. NMR data obtained as a function of the temperature point to an equilibrium of type a in solution.

In order to verify this hypothesis a small quantity of H_2 gas was bubbled into the NMR tube containing **1** (in $CDCl_3$). The intensity of the broad signal at $\delta \approx 2.5$ ppm in the ^1H NMR spectrum strongly increased, while the hydride signals underwent a strong paramagnetic shift ($\sim$5 ppm) and broadened from 4 to 50 Hz, indicating equilibrium shifts toward species A. When D_2 gas was bubbled into the NMR tube, the broad peak at $\sim$2.5 ppm disappeared. However, when H_2 was bubbled into a NMR tube containing $CDCl_3$ only, a sharp peak appeared at 4.61 ppm, which disappeared in 60 s.

In compound **2** the broad peak at $\delta \approx -0.4$ ppm can be attributed to H_2 bonded to the metal center.[21] In fact when H_2 is bubbled in the solution, the hydrido peak at $\delta = -47.9$ ppm broadens and shifts to $\sim$−46 ppm while the already broad peak at $\sim$−0.4 ppm disappears; this may be due to a paramagnetic shift leading this weak resonance to the crowded 1–2 ppm region or to extreme broadening, but in any case it involves chemical exchange between free and bonded H_2. The above behavior is observed for the peak at $\sim$−0.4 ppm, when the temperature is lowered.

Thus, the proposed equilibrium (a) would appear to be consistent with and rationalize all solution and solid-state data.[10] The likely explanation of why the molecular H_2 formed in (a) does not leave the solution is that H_2 is coordinated to the monohydrido species B, as has recently been reported for other complexes.[21,22]

It is conceivable that an intermediate of the type $\{B\text{–}H_2\}$ reacts with a second molecule of B, giving e.g. a transition state of the type $\{B\text{–}H_2\text{–}B\}^*$, which than splits into two molecule of A. From this point of view the A → B transformation of equilibrium b could be seen as an example of a temperature-dependent, reversible ligand-to-metal charge transfer (LMCT)[23] while the reverse process would correspond to a metal-to-ligand charge transfer (MLCT).

$$2[Ir^{IV}(H)_2(Cl)_2(PR_3)_2] \underset{MLCT}{\overset{LMCT}{\rightleftharpoons}} [Ir^{III}(H)(Cl)_2(PR_3)_2]_2{\cdot}H_2 \quad (b)$$

Although a fairly concentrated (8×10^{-3} M) $CHCl_3$ solution of **1** does not show an EPR signal when cooled to 193 K,[11] a much more concentrated solution of **1** (5×10^{-2} M) shows a detectable EPR spectrum[18] when cooled to 95 K. The g values (2.064, 2.038, 2.007) are in agreement with a quasi-isotropic, slightly distorted octahedral geometry of Ir(IV). No hyperfine structure was observed.

Although we are unable to measure the amount of the paramagnetic compound responsible for the EPR signal, which we postulate to be A, that is present in solution, we can say that it is very small, considering the conditions of the measurement (modulation amplitude 2.5 G, receiver gain 1000). Thus, EPR measurements confirm the paramagnetic diamagnetic equilibrium, proposed on the basis of the NMR study.

$CHCl_3$ solutions of **2** (5×10^{-2} M) when cooled to 95 K show a quasi-isotropic spectrum; the signals observed in the solid-state spectrum are not present.[18] Also for compound **2** the g values (2.064, 2.040, 2.008; modulation amplitude 2.5 G, receiver gain 500) are in agreement with a quasi-isotropic, slightly distorted octahedral geometry of Ir(IV). As for compound **1**, no hyperfine

(21) (a) Crabtree, R. H.; Lavin, M.; Bonneviot, L. *J. Am. Chem. Soc.* **1986**, *108*, 4032–4037 and references cited therein. (b) Kubas, G. J.; Unkefer, C. J.; Swanson, B. I.; Fukushima, E. *J. Am. Chem. Soc.* **1986**, *108*, 7000–7009 and references cited therein.

(22) (a) Kubas, G. J.; Ryan, R. R.; Swanson, B. I.; Vergamini, P. J.; Wasserman, H. J. *J. Am. Chem. Soc.* **1984**, *106*, 451–452. (b) Upmacis, R. K.; Gadd, G. E.; Poliakoff, M.; Simpson, M. B.; Turner, J. J.; whyman, R.; Simpson, A. F. *J. Chem. Soc., Chem. Commun.* **1985**, 27–30 and references cited therein. (c) Hay, P. J. *J. Am. Chem. Soc.* **1987**, *109*, 705–710 and references cited therein.

(23) Sohn, Y. S.; Hendrickson, D. N.; Gray, H. B. *J. Am. Chem. Soc.* **1971**, *93*, 3603–3612.

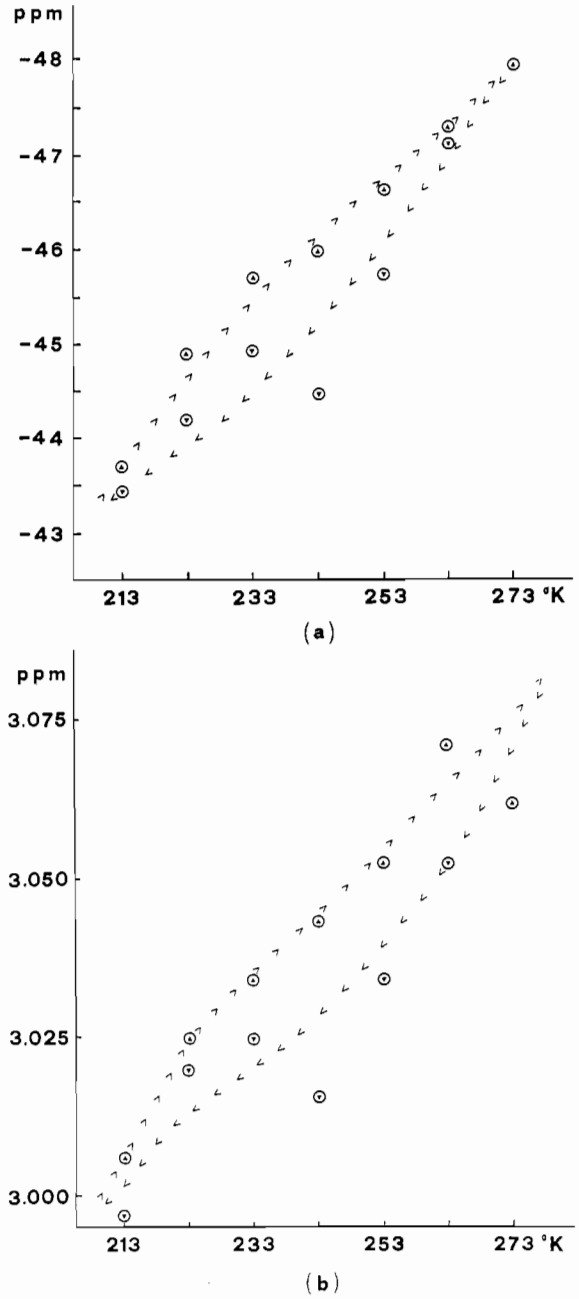

Figure 4. Chemical shift behavior as a function of the temperature for the hydrido peak (a) and for the methyne peak (b) in the 200-MHz ^1H NMR spectrum of **1**. In each case the measurements were made by starting from the lowest temperature. (The peak due to the methyl groups does not shift enough.)

structure was observed for **2**. The same interpretation concerning the quantity of paramagnetic species in solution made for **1** can be extended to complex **2**. Thus, the behavior of compound **2** gives further evidence of the existence of the equilibrium shown in reactions a and b.

Conclusions

In our opinion compounds **1** and **2** are not isolated examples. Considering the extremely large chemical shifts (~−50 ppm) reported by Shaw et al.,[24] as well as by Werner et al.,[25] for several monohydrido Ir(III) complexes and given the similarity between the chemical shifts of **1** and **2** (δ(Ir−H) = −49.0 and −47.9 ppm) and those of the Shaw and Werner compounds, it is possible that

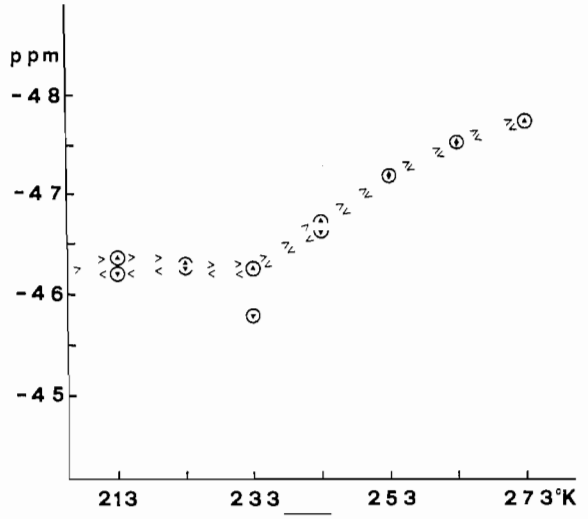

Figure 5. Chemical shift behavior as a function of the temperature for the hydrido peak in the 200-MHz ^1H NMR spectrum of **2**. The measurements were made by starting from the lowest temperature. (The peaks due to the methyne and methylene groups do not shift enough.)

Table V. Crystal Data for $Ir^{IV}(H)_2(Cl)_2(P\text{-}i\text{-}Pr_3)_2$ (**1**)

formula	$C_{18}H_{44}Cl_2P_2Ir$
mol wt	585.66
cryst dimens, nm	0.13 × 0.23 × 0.68
cryst syst	monoclinic
space group	$P2_1/c$
a, Å	8.191 (3)
b, Å	8.982 (4)
c, Å	16.447 (4)
β, deg	93.30 (2)
V, Å^3	1208.0 (7)
Z	2
calcd density, g cm^{-3}	1.61
measd density,[b] g cm^{-3}	1.60 (1)
scan method	$\theta/2\theta$
radiation	Mo Kα (λ = 0.71069 Å)
monochromator	graphite cryst
2θ range, deg	3–90
octants collected	$+h,\pm k,\pm l$
no. of total data	13582
variable scan speed range, deg min^{-1}	1.0–29.3
no. of obsd data, $I_o > 3\sigma(I_o)$	5237
R value for equiv reflns	0.0304
μ, cm^{-1}	62.13
F(000)	586.0
final residuals (for 5237 data)	
R_F, R_{wF}	0.0312, 0.0360
weighting scheme	$(\sin\theta)/\lambda$
goodness of fit for last cycle	0.90
max $\Delta\sigma$ for last cycle	0.01

[a] Lattice constants calculated from 15 high-angle reflections measured at $\pm 2\theta$ (2θ interval 37.65–51.29°). [b] Measured by flotation in $CdCl_2$ aqueous solution.

their behavior is analogous to that which we observe for **1** and **2**. Consequently, paramagnetic hydrido complexes may be present in solution.

Furthermore, we also think that the same hypothesis could be extended to the rhodium hydride analogues prepared by Shaw et al.,[26] considering the high-field chemical shifts that they show, for which we suggest a structure isomorphous with that of the iridium compounds.

Experiments are in progress to test this hypothesis.

Experimental Section

Materials and Equipment. All the starting materials and solvents used were commercially available. The syntheses were done under oxygen-free nitrogen. Infrared spectra were obtained with a Perkin-Elmer 983G spectrophotometer. ^1H and ^{31}P NMR spectra were recorded on a Bruker

(24) (a) Masters, C.; Shaw, B. L.; Stainbank, R. E. *J. Chem. Soc. D* **1971**, 209. (b) Masters, C.; Shaw, B. L.; Stainbauk, R. E. *J. Chem. Soc. A* **1971**, 664–666. (c) Shaw, B. L.; Stainbank, R. E. *J. Chem. Soc., Dalton Trans.* **1972**, 2108–2112.

(25) Werner, H.; Wolf, J.; Hohn, A. *J. Organomet. Chem.* **1985**, *287*, 395–407.

(26) Master, C.; Shaw, B. L. *J. Chem. Soc. A* **1971**, 3679–3686.

Table VI. Crystal Data for $Ir^{IV}(H)_2(Cl)_2(PCy_3)_2$ (**2**)

formula	$C_{36}H_{68}Cl_2P_2Ir$
mol wt	826.08
cryst dimens, mm	0.15 × 0.18 × 0.29
cryst syst	triclinic
space group	$P\bar{1}$
cell dimens[a]	
a, Å	10.003 (4)
b, Å	10.288 (6)
c, Å	10.708 (4)
α, deg	113.06 (4)
β, deg	109.23 (3)
γ, deg	91.77 (4)
V, Å^3	940.9 (7)
Z	1
calcd density, g cm^{-3}	1.46
scan method	$\theta/2\theta$
radiation	Mo Kα (λ = 0.71069 Å)
monochromator	graphite cryst
2θ range, deg	3–56
octants collected	$\pm h,\pm k,\pm l$
no. of total data	10425
variable scan speed range, deg min^{-1}	1.2–29.3
no. ov obsd data, $I_o > 3\sigma(I_o)$	4863
R value for equiv reflns	0.0228
μ, cm^{-1}	40.14
$F(000)$	425.0
final residuals (for 4863 data)	
R_F, R_{wF}	0.0181, 0.0247
weighting scheme	$(\sin\theta)/\lambda$
goodness of fit for last cycle	1.17
max Δ/σ for last cycle	0.00

[a] Lattice constants calculated from 15 high-angle reflections measured at $\pm 2\theta$ (2θ interval 35.58–51.54°).

AC200 instrument.[27] EPR spectra were recorded on a Varian E-9 spectrometer. Magnetic susceptibility measurements were made with three different balances: (a) an Oxford Instruments apparatus equipped with a Cahn 2000 microbalance; (b) an Oxford Instruments apparatus equipped with two superconducting solenoids and with a Sartorius electronic vacuum microbalance; (c) a Gouy balance (6500-G permanent magnet).

Synthesis of $Ir^{IV}(H)_2(Cl)_2(P\text{-}i\text{-}Pr_3)_2$ (1). One gram of $(NH_4)_2IrCl_6$ was suspended in 11 mL of ethanol, containing 1.4 mL of concentrated HCl. The suspension was heated under reflux until the color changed to dark gray (about 2 h). After removal of heat, 1.2 mL of P-*i*-Pr_3 in 5 mL of degassed ethanol was added to the above suspension with vigorous stirring. The suspension was heated under reflux for 4 h. During this period the color of the suspension changed from gray to yellow-gray and then to gray-green. Looking at the suspension with a light, it is possible to recognize the presence of a gray-green solid and red microcrystals. The suspension was filtered; the mixture that remained on the filter was first dried under vacuum and then washed several times with H_2O (5 × 10 mL). The gray-green solid dissolved, leaving the deep purple microcrystals on the filter. No further purification was necessary; yield 0.41 g (31%, based on $(NH_4)_2IrCl_6$).

Synthesis of $Ir^{IV}(H)_2(Cl)_2(PCy_3)_2$ (2). One gram of $(NH_4)_2IrCl_6$ was suspended in 11 mL of ethanol, containing 1.4 mL of concentrated HCl. The suspension was heated under reflux until the color changed to dark gray (about 2 h). After removal of heat, 2.1 g of PCy_3 in 10 mL of ethanol was added to the above suspension with vigorous stirring. The suspension was heated under reflux for 4 h. During this period the color of the suspension changed from grey to yellow-gray and then to gray-green and finally to pink-red. The suspension was filtered; the mixture that remained on the filter was first dried under vacuum and then washed several times with H_2O (5 × 10 mL). After this treatment a red-violet compound remained on the filter. No further purification was necessary; yield 1.05 g (56.1%, based on $(NH_4)_2IrCl_6$).

X-ray Structure Solution and Refinement. $Ir^{IV}(H)_2(Cl)_2(P\text{-}i\text{-}Pr_3)_2$ (1). Deep red crystals of **1** were obtained from benzene solution in the form of prisms and were air stable. Data collection was performed by a Nicolet P3m automatic diffractometer (room temperature); the data were corrected as described in ref 28. The structure was solved by heavy-atom techniques and refined as a full matrix in least-squares calculation using local programs.[29] The number of observations was 5237 ($I > 3\sigma(I)$), and the number of variable parameters was 190 (27.6 observations for each parameter). A difference Fourier synthesis, based on low-angle reflections[30] (maximum $(\sin\theta)/\lambda$ = 0.36 Å^{-1}), clearly revealed the hydrido hydrogen positions (the residual electron density for the hydride hydrogen in the difference-Fourier synthesis is 0.60 (9) Å^{-3}). Full-matrix refinement of all heavy atoms (anisotropic thermal parameters) and hydrido hydrogens (isotropic thermal parameters) with fixed contributions of 21 H atoms of the P-*i*-Pr_3 group gave R_F = 0.0158 and R_{wF} = 0.0180 (with 458 reflections for 113 parameters).

The final R_F values of observed reflections (full-matrix refinement) after introduction of the hydride hydrogen (coordinates and isotropic temperature factor fixed), with the full set of 5237 reflections, are R_F = 0.0312 and R_{wF} = 0.0360. An extinction parameter was not used because a check of the observed and calculated structure factors suggested that it was unnecessary.

Additional details of the crystallographic experiments concerning **1** are given in Table V.

$Ir^{IV}(H)_2(Cl)_2(PCy_3)_2$ (2). The data obtained from a red prism of **2** (crystallized from benzene solution) were treated as those of **1**. The number of observations was 4863 ($I > 3\sigma(I)$), and the number of variable parameters was 319 (15.2 observations for each parameter). A difference Fourier synthesis, based on low-angle reflections[30] (maximum $(\sin\theta)/\lambda$ = 0.36 Å^{-1}), clearly revealed the hydrido hydrogen positions (the residual electron density for the hydride hydrogen in the difference-Fourier synthesis is 0.24 (4) Å^{-3}). Full-matrix refinement of all heavy atoms (anisotropic thermal parameters) and hydrido hydrogens (isotropic thermal parameters) with fixed contributions of 33 H atoms of the PCy_3 group gave R_F = 0.0099 and R_{wF} = 0.0116 (with 738 reflections for 191 parameters); the large B_{iso} value of the H(111) atom (see Table II) suggests that the hydride hydrogen is disordered in the $P\bar{1}$ space group. Therefore, we carried out the refinement of the structure in the $P1$ space group. The refinement was unsuccessful; then we decided definitively to choose the $P\bar{1}$ space group. The final R_F values of observed reflections (full-matrix refinement) after introduction of the hydride hydrogen (coordinates and isotropic temperature factor fixed), with the full set of 4863 reflections, are R_F = 0.0181 and R_{wF} = 0.0247. An extinction parameter was not used because a check of the observed and calculated structure factors suggested that it was unnecessary.

Additional details of the crystallographic experiment concerning **2** are given in Table VI.

Neutral-atom scattering factors and corrections for anomalous dispersion were from ref 31.

Magnetic Measurement of Compound 1. The μ_{eff} value was measured for the powdered sample (298 K) by the Gouy method (tube calibrated with $NiCl_2$ solution); the magnetic susceptibility was confirmed by the Faraday method with use of two different instruments. A diamagnetic correction[32] was carried out. Both methods give μ_{eff} = 1.5 (1) μ_B.

Magnetic Measurement of Compound 2. The μ_{eff} value was measured for the powdered sample (298 K) by using the Faraday method, with two different instruments. A diamagnetic correction[32] was carried out. Both balances give μ_{eff} = 1.6 (1) μ_B.

Acknowledgment. We are indebted to Prof. L. M. Venanzi for valuable suggestions and discussions. We also thank Dr. D. Fiorani, Dr. M. Gardini,[33] and F. De Zuane[34] for magnetochemical measurements.

Supplementary Material Available: Thermal parameters of non-hydrogen atoms (Table A) and hydrogen atomic parameters with isotropic thermal parameters (Table B) for $Ir^{IV}(H)_2(Cl)_2(P\text{-}i\text{-}Pr_3)_2$ (**1**) and thermal parameters of non-hydrogen atoms (Table D) and hydrogen atomic parameters with isotropic thermal parameters (Table E) for $Ir^{IV}(H)_2(Cl)_2(PCy_3)_2$ (**2**) (4 pages); observed and calculated structure factors for **1** (Table C) and **2** (Table F) (51 pages). Ordering information is given on any current masthead page.

(27) NMR spectra were collected at the NMR service of the Research Area of Rome.
(28) Bachechi, F.; Zambonelli, L.; Marcotrigiano, G. *J. Cryst. Mol. Struct.* **1977**, *7*, 11–20.
(29) Camalli, M.; Capitani, D.; Cascarano, G.; Cerrini, S.; Giacovazzo, C.; Spagna, R. "SIR CAOS", Ital. Patent 35403c/86, 1986; *User Guide*; Istituto di Strutturistica Chimica CNR: C.P. 10, 00016 Monterotondo Stazione, Rome, Italy.
(30) Bau, R.; Chiang, M. Y.; Ho, D. M.; Gibbons, S. G.; Emge, T. J.; Koetzle, T. F. *Inorg. Chem.* **1984**, *23*, 2823–2829 and references cited therein.
(31) *International Tables for X-ray Crystallography*; Kynoch: Birminghan. England, 1974; Vol. 4.
(32) O'Connor, C. J. Magnetochemistry-Advances in Theory and Experimentation. In *Progress in Inorganic Chemistry*; Lippard, S. J., Ed.; Wiley: New York, 1982; Vol. 29, 208–211.
(33) Istituto di Teoria e Struttura Elettronica e Comportamento Spettrochimico dei Composti di Coordinazione. CNR, Rome, Italy.
(34) Istituto di Chimica e Tecnologia dei Radioelementi CNR, Padova, Italy.